Unraveling the thermodynamics of the CO<inf>2</inf> driven precipitation of cellulose in aqueous NaOH

Citation for the original published paper (version of record):
Karna, N., Kozlowski, A., Hasani, M. (2023). Unraveling the thermodynamics of the CO<inf>2</inf> driven precipitation of cellulose in aqueous NaOH. Chemical Physics, 575. http://dx.doi.org/10.1016/j.chemphys.2023.112060

Chemical Physics 575 (2023) 112060

Contents lists available at ScienceDirect

Chemical Physics

journal homepage: www.elsevier.com/locate/chemphys

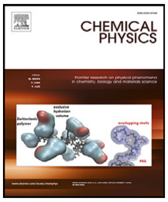

Unraveling the thermodynamics of the CO_2 driven precipitation of cellulose in aqueous NaOH

Nabin Kumar Karna [a,b,*], Alexandra Maria Kozlowski [a], Merima Hasani [a]

[a] Chalmers Univesity of Technology, Kemigården 4, Gothenburg, 41296, Sweden
[b] Wallenberg Wood Science Center, KTH Royal Institute of Technology, Stockholm, SE-10044, Sweden

ARTICLE INFO

Keywords:
Cellulose
Thermodynamics
Precipitation
Carbon dioxide
Aggregation
Molecular dynamics

ABSTRACT

Hypothesis: The incorporation of carbon dioxide into a sodium hydroxide solution containing cellulose may induce the formation of a transient cellulose carbonate intermediate, which readily hydrolyzes to carbonate ion, and this process is responsible for the instantaneous formation of loose cellulose aggregates.
Simulations: We employed molecular dynamics simulations to gain insight into the role of carbon dioxide and related ions in the cellulose aggregation process. By performing free energy calculations using OPLS/AA force fields between cellulose chains at different ionic environments, we were able to gain additional information regarding the behavior and thermodynamics of the involved species and propose a potential mechanism for the aggregation of cellulose in these systems.
Findings: Our hypothesis of the formation of an intermediate cellulose carbonate in the solution, which strongly favors carbon dioxide absorption and carbonate ion formation, is supported by the simulation results. These results suggest that the aggregation process is driven by entropy upon the introduction of carbonate ions into the system.

1. Introduction

In the quest for a sustainable cellulose solvent, aqueous hydroxide bases have emerged as promising contenders. Among them, NaOH(aq) is favored for its green nature, general availability, and low toxicity. However, the dissolution scope of cellulose in pure sodium hydroxide, without additives, is limited. The implications of poor solubility have been extensively explored with regards to NaOH(aq) concentration, temperature, as well as cellulose chain length, character, or origin [1–4]. The interaction between cellulose and CO_2(g), which is present in the solution as a result of natural sorption by NaOH(aq), has been largely ignored for a significant period of time [5–8], we previously showed that the presence of cellulose significantly increases the incorporation of CO_2 into the system [9]. Interestingly, the increased incorporation of CO_2(g) was accompanied by a relatively modest reduction of alkalinity and pointed out the hydroxide-preserving nature of carbonate formation (as compared to the common alkali mediated conversion of CO_2) [9]. Following NMR studies of low-molecular cellulose analogues evidenced the critical role of the carbohydrate in the CO_2(g) uptake whilst insensitivity of the process to variations in alkali concentrations [10]. Based on these findings we could suggest a mechanism for introducing CO_2(g) through a formation of transient cellulose carbonate intermediate, readily hydrolyzed to yield a carbonate ion. Even though the intermediate mentioned above could not be captured by NMR in an aqueous alkaline environment, its formation under similar conditions was reported in early carbohydrate literature [11,12] as well as in the DMSO system [13]. Importantly, CO_3^{2-} formation route would account for a modest reduction of alkalinity, as it comprises consumption of only one mole OH^- per mole of formed CO_3^{2-}, contrary to the classical route consuming 2 moles of OH^- per mole of formed CO_3^{2-}. By building knowledge on the interaction between cellulose and CO_2(g) in cold alkali, we could take control of the system and investigate further the polymer behavior in the context of material development. Recently, we reported the remarkable ability of the introduced CO_2(g) to precipitate cellulose from NaOH(aq) while largely preserving the alkalinity: cellulose could be precipitated by CO_2(g) with the reduction in alkalinity corresponding to merely 0.3 pH units at 5 °C [14]. Following this, the uptake of CO_2(g) for the colloidal stability of the cellulose/NaOH(aq) solutions was emphasized in the studies by Reyes et al. [15] comprising cellulose dissolution under a CO_2(g)-depleted atmosphere and ageing of solutions in contact with CO_2(g). Although both our work and consecutive research of Reyes et al. [16] hypothesized on the coagulation mechanism, there is still a lack of complete mechanistic understanding. Due to the complexity and harsh conditions in the studied system, as well as rapid change whilst gas delivery, the analytical techniques that

---

[*] Corresponding author at: Chalmers Univesity of Technology, Kemigården 4, Gothenburg, 41296, Sweden.
E-mail address: nabin@chalmers.se (N.K. Karna).

https://doi.org/10.1016/j.chemphys.2023.112060
Received 30 April 2023; Received in revised form 26 July 2023; Accepted 21 August 2023

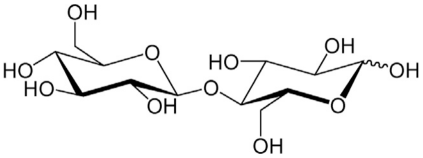

Fig. 1. Schematic representation of cellobiose unit.

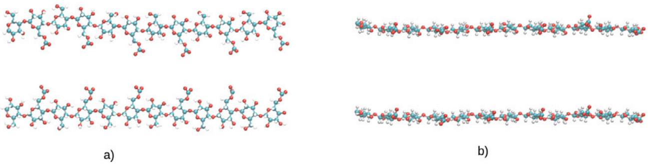

Fig. 2. Schematic representation of the hydrophilic (left) and hydrophobic (right) sides of cellulose chains used in this study. The figure shows the interacting sides of the cellulose carbonate chains, while similar sides have been chosen to study the interaction between the deprotonated chains.

could support the presented reasoning are limited. In light of that, molecular modeling could be a door opener toward a complete picture of the coagulation mechanism. The essence of such an approach is to appropriately reflect the experimental environment, including the polymeric structure of celluloses, rather than the analysis of a single glucose unit. Here, therefore, we employ molecular dynamics simulations to attain a mechanistic understanding of cellulose aggregation in NaOH solution in the presence of CO_2.

2. Methodology

A series of MD simulations have been conducted using GROMACS2022, an MD package that has widely been used to investigate the molecular interaction phenomena for systems involving biomolecules [17–19]. A time step of 2 fs (2×10^{-15} s) was used in all MD simulations. A cut-off distance of 1 nm was implemented for truncating the van der Waals force in our study. Long-range electrostatic interactions were calculated using Smooth Particle Mesh Ewald (SPME) method [20]. All the equilibration and production simulations were carried out in NPT ensemble at 300 K, unless otherwise mentioned. The temperature was controlled using velocity rescaling version [21] of Berendsen thermostat [22] with a time constant of 0.1 ps to isolate athermal effects as much as possible [23–25] and periodic boundary condition were applied in all directions throughout all the simulations. The pressure was maintained at 1 atm by using a semi-isotropic Berendsen barostat in x and y directions. Cellulose 1β crystals were modeled with chains formed by repeating cellobiose units as shown in Fig. 1 based on the structure predicted by Nishiyama et al. [26] Two types of cellulose chains viz. carbonated and deprotonated, were used in this study. The carbonated cellulose chains were constructed by substituting H6 atoms of alternate cellobiose units with a carbonate group. Electrostatic charges on C6 and HO6 were adjusted on each substituted unit such that the effective charge of the modified unit was −2. Similarly, the deprotonated cellulose chains were constructed by removing the H6 atoms from the alternate cellobiose units and adjusting charges in C6 and HO6 atoms, so that the overall effective charge of the deprotonated unit was −1.

Numerous force-fields like AMBER [27], CHARMM [28], and GROMOS [29] among others have been reported for carbohydrate systems, we chose to implement OPLS/AA FF, which has been reported to be consistent with the larger biomolecular context. This force field has also been employed in condensed-phase simulations of cellulose in aqueous media in previous studies and has been proven to successfully predict the interaction between different faces of nanocrystalline cellulose [30]. Water molecules were described using the simple point charge SPC/E model [31] which has successfully been used in studies involving water-cellulose systems [32]. We have chosen the SPC/E water model due to its quantitative agreement with experiments to yield water reorientation and hydrogen bond (HB) dynamics [33]. Moreover, it has been shown that the value of the surface tension for the SPC/E model is in good agreement with the experimental results [34].

Two cellulose chains composed of 6 cellobiose units, as shown in Fig. 1, were placed in a computational domain of 2.4 nm × 6.00 nm × 6.228 nm^3. The computational box was then filled with a fixed number of water molecules and free sodium ions were used to neutralize the surplus charge in the system created due to cellulose modification (deprotonation and carbonation). Subsequently, an adequate number of sodium and hydroxide ions were introduced to generate a system of 1 molar NaOH concentration. For the cases involving CO_2 and CO_3^{-2} adequate number of carbon dioxide or carbonate ions were introduced to generate 1 molar concentration of each species. The additional charges created in the system due to the addition of ionic species were further neutralized by adding sodium ions.

In all the simulations, the systems were first energy minimized and then subjected to NVT ensemble at 300 K for 5 ns and subsequently to NVE ensemble for the next 20 ns to guarantee the equilibrium properties of the involved species. Then, the systems were subjected to NPT ensemble for further equilibration and production runs. The interspecies interaction parameters were described using Lorentz-Bertholet (LB) mixing rules [35].

The magnitude of interactions between the modified cellulose chains was calculated using umbrella sampling (US) and the weighted histogram analysis method (WHAM) [36], where the latter was used to calculate the potential of mean force (PMF) along a reaction coordinate. In our case, the reaction coordinate was chosen to be the interparticle separation of the center of mass (COM) of each cellulose chain. A chain of the cellulose (Chain A) was rendered fixed by applying position restraints of 500 kJ mol^{-1} nm^{-2} on each carbon atom in all three directions. Similarly, the next chain (Chain B) was rendered mobile in the direction of the reaction coordinate (z-axis) by applying position restraints of 500 kJ mol^{-1} nm^{-2} to all the carbon atoms in the x and y directions. This was done to prevent its rotation along the x-y plane and ensure a fixed orientation during the pulling process. The US was started by initially pulling Chain B towards Chain A, at a constant rate of 0.0025 nm ps^{-1} with a force constant of 10,000 mol^{-1} nm^{-1}. The system configurations were stored at 0.05 nm intervals, which were used for the US. The sampling time of 6 ns was used for all configurations.

Entropy was calculated from the finite difference temperature derivative of PMF or ΔG at each interparticle separation (r) using Eq. (1):

$$-\Delta S(r) = \frac{\Delta G(r, T + \Delta T) - \Delta G(r, T)}{\Delta T} \tag{1}$$

PMF calculation using the US method was conducted at 300 K and 320 K and hence, the values of T and ΔT were 300 K and 20 K, respectively. The enthalpic contribution to the free energy, ΔH, can be then calculated using Eq. (2):

$$\Delta H = \Delta G + T\Delta S \tag{2}$$

3. Results and discussion

3.1. Interaction between cellulose chains

The interactions between two cellulose chains were determined by calculating the PMF between them in the presence and absence of the ions of interest. The PMFs of most relevant cases were further decomposed into their entropic and enthalpic contributions to explore the main reason behind the experimentally observed [14] cellulose aggregation in presence of CO_2 in NaOH. The PMF profiles between the hydrophilic sides of the depronoted cellulose chains in different

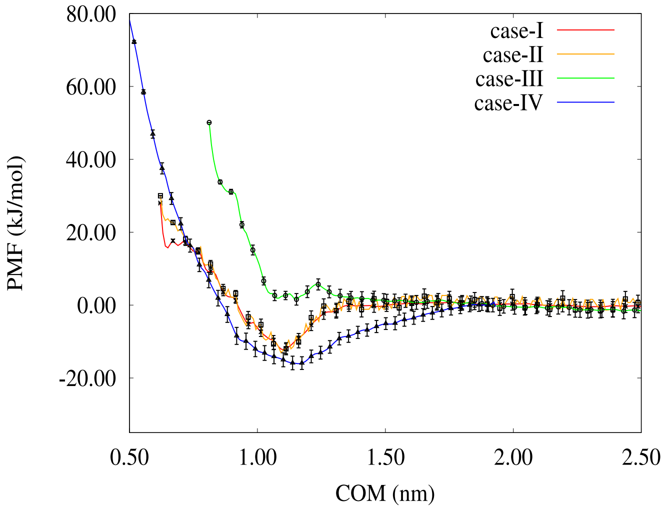

Fig. 3. PMF profile of interaction between the hydrophilic sides of two deprotonated cellulose chains. The labels in the figure is as follows: (i) case I: Water without OH^-, CO_2 or CO_3^{-2}, (ii) case II: Solution with CO_2 concentration of 1 molar in water, (iii) case III: Water with OH^- concentration of 1 molar and no CO_3^{-2}, (iv) case IV: Water with OH^- concentration of 1 molar and CO_3^{-2} concentration of 1 molar.

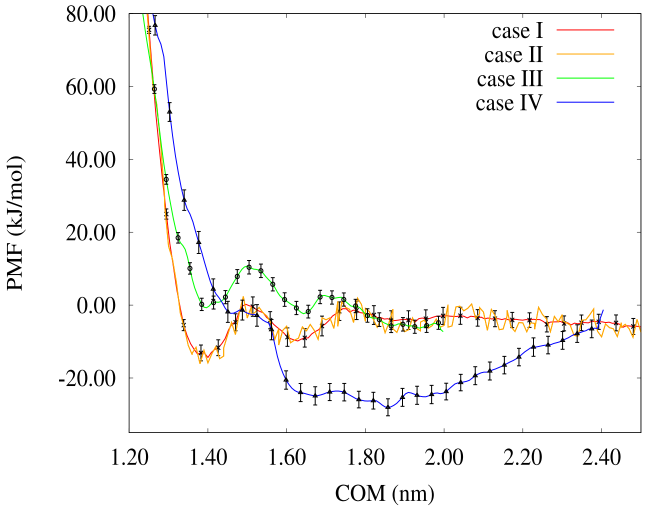

Fig. 4. PMF profiles of interaction between the hydrophilic sides of two carbonated cellulose chains. The labels in the figure are as follows: (i) case I: Water without OH^-, CO_2 or CO_3^{-2}, (ii) case II: Solution with 1 molar CO_2 in water, (iii) case III: Water with OH^- concentration of 1 molar and no CO_3^{-2}, (iv) case IV: Water with OH^- concentration of 1 molar and CO_3^{-2} concentration of 1 molar.

solutions are shown in Fig. 3. The interaction between the chains in water seems not to be affected by the presence of gaseous CO_2 in the solution as shown by the PMF profiles (cases I and II). It has previously been shown that the PMF profiles between two interacting cellulose chains depend upon the orientation of water molecules in the interfaces [17]. The similarity in PMF profiles in these two cases suggests that the water structure is very weakly affected by CO_2 in water and does not change significantly [37]. On the other hand, the PMF profiles for high concentration of OH^- ions (cases III and IV) reveal primary maxima prior to primary minima, which indicates the existence of an energy barrier that prevents the association of deprotonated cellulose chains under such conditions. Having shown that the presence of gaseous carbon dioxide does not alter the PMF profiles of the interacting chains, we now focus on the effect of carbon dioxide in the solution. It is well known that carbon dioxide is absorbed in NaOH solutions and forms stable carbonate ions [38]. Furthermore, our previous study [14] has shown that dissolved cellulose chains in NaOH(aq) solution may assist in higher absorption of CO_2 from the atmosphere. One of the possible explanations for this observation is the formation of a cellulose carbonate intermediate, readily hydrolyzed to carbonate ion, as suggested by Gunnarson et al. [13] To this end, we first study the effect of the presence of CO_3^{-2} species in the solution containing Na^+ and OH^- ions and water (cases III and IV, (Fig. 3). We introduce an adequate number of CO_3^{-2} species into the solution to generate 1 molar concentration and neutralize the system charge by further adding Na^+ ions. The PMF profile of the deprotonated chains, in this case, indicates the presence of deep primary minima that is deeper and wider than the case without any OH^- ions which indicate the formation of instantaneous cellulose aggregates.

Subsequently, we introduce the carbonate species on the cellulose chains to simulate cellulose carbonate in solution and calculate the corresponding PMF profiles (Fig. 4). It is worth noting that the PMF profiles of deprotonated cellulose chains in water differ from those of carbonated chains despite both having the same overall charge on the interacting sides (cf. Figs. 3 and 4). For example, in the case I described in Fig. 4, (carbonated cellulose chains without deprotonation) secondary minima are observed before the primary maxima when the interacting faces of the carbonated chains come closer to one another. This implies that aggregation of carbonated cellulose chains is less likely compared to the aggregation of the deprotonated chains, as the carbonated chains are likely to attain a stable state at the secondary minima; the energy barrier to overcome for the system to be in this local minimum energy state being $\sim 4kT$. This suggests that modification of cellulose chains by a charged substituent leads to higher stability of cellulose suspensions and prevents aggressive aggregation [39]; compared to the deprotonated chains without substitution. The presence of only primary minima in the PMF profiles of deprotonated chains in water (without OH^- and CO_3^{-2} ions) indicates that these chains are more likely to form stable aggregates under favorable conditions.

However, in the presence of base, this seems to change. The PMF profiles between the hydrophilic sides of two carbonated cellulose chains in different systems containing CO_2, OH^- and CO_3^{-2} are shown in Fig. 4. Similar to the case with deprotonated cellulose chains in presence of gaseous carbon dioxide in water, the PMF profiles, in this case, show no significant variation upon addition of gaseous CO_2. This strongly suggests that free gaseous CO_2 does not significantly affect the aggregation process. The presence of NaOH in the system increases the primary free energy barriers and the minima of the PMF profiles are less deep which indicates a lower probability of aggregation of cellulose chains in the presence of NaOH. The introduction of CO_3^{-2} however, drastically affects the free energy of the system, as shown in Fig. 5. The region with the secondary maxima disappears altogether and only wide and deep minima are observed; although a small repulsive barrier is still observed, approximately in a similar region where primary maxima were observed for other cases. The presence of deeper primary minima in the PMF profile suggests a high probability of instantaneous aggregation without any resistance. However, the deeper region of primary minima, in this case, lies further away from the COM of the chains compared to the other cases, which indicates the formation of looser aggregates, and not permanent precipitation. This trend is similar to case III discussed in Fig. 3.

To further investigate this interesting tendency of aggregation in the presence of CO_3^{-2}, we calculate the enthalpic and entropic contribution in the cases with both OH^- and CO_3^{-2} in the system. The respective entropic and enthalpic contributions are shown in Figs. 5 and 6 for the systems with deprotonated and carbonate cellulose chains respectively. The enthalpic and the entropic contributions of the PMF act in opposite direction to one another and depends upon the interparticle distance of the cellulose chains. The aggregated state of the chains is highly favored due to the huge entropic contributions, the enthalpic contributions

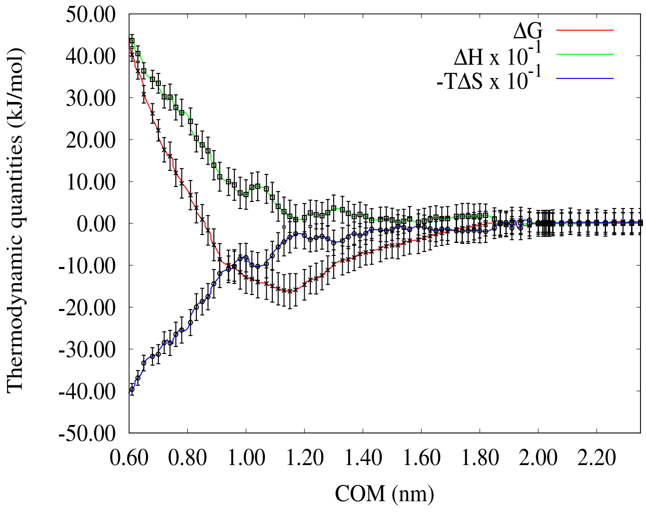

Fig. 5. Enthalpic contribution, $\Delta H(r)$, and entropic contribution, $-T\Delta S(r)$, to the potential of mean force, $\Delta G(r)$ for the system with deprotonated cellulose chains in water along with OH^- and CO_3^{-2} ions. It is to be noted that the interaction between the hydrophilic sides are only considered in the system.

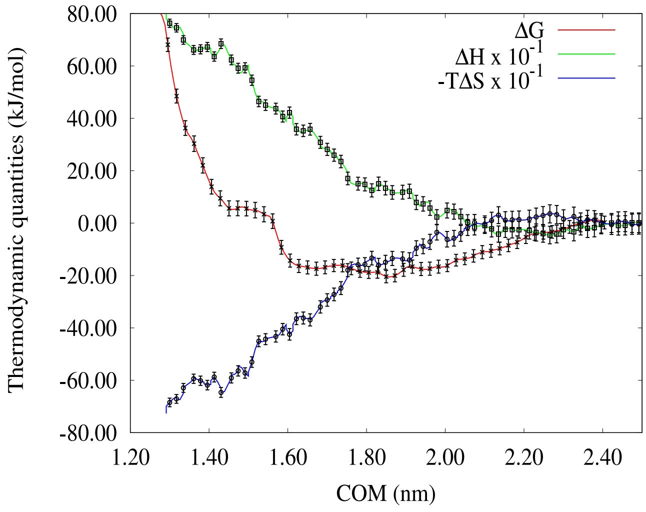

Fig. 6. Enthalpic contribution, $\Delta H(r)$, and entropic contribution, $-T\Delta S(r)$, to the potential of mean force, $\Delta G(r)$ for the system with carbonated cellulose chains in water along with OH^- and CO_3^{-2} ions. It is to be noted that the interactions between the hydrophilic sides are only considered in the system.

being unfavorable. This suggests that the observed change in free energy which gives rise to attractive minima is particularly due to an increase in the entropy of the system which might be the result of the rearrangement of water molecules in the solvation layer of the carbonate ions and the expulsion solvent molecules between the cellulose chains. We observe that the minimum energy state; i.e. the primary minima, is stabilized by increased entropy, while beyond the primary minima, at the lower interparticle separation, the interaction is dominated by higher enthalpic contribution. This suggests higher intermolecular interaction among the water molecules trapped between the cellulose chains as the latter approach one another closer than the primary minima.

It is to be noted that the contact minimum of the system with carbonated chains is deeper and wider as compared to the system with deprotonated chains only, despite both systems having the same numbers of ionic species and water molecules. This suggests that the presence of carbonated cellulose chains contributes to the deeper energy by increasing the entropy of the system which in turn leads to a higher probability of cellulose chain aggregation. This finding explains the formation of cellulose aggregates in NaOH solution in the presence of CO_2. Furthermore, the larger gain in entropy at the minimum energy state observed in the case of a system with cellulose carbonate chains and a higher uptake of CO_2, as experimentally shown in our previous investigation [14] hints towards the presence of cellulose carbonate species, albeit transient, during the uptake of CO_2 from the atmosphere by the cellulose dissolved in NaOH solution. Although we focus our results and discussions around the interaction between the hydrophilic sides of the cellulose chains (Fig. 2), we have performed similar analyses for the hydrophobic sides, included as supplementary information. The aggregation tendency of the hydrophobic sides shows similar trends as the interaction between the hydrophilic sides, which suggests that the aggregation tendency of the cellulose chains does not depend upon the interacting sides, but on the presence of CO_3^{-2} ions in the system.

Concluding remarks

The theoretical results obtained via MD simulation reveal that the presence of CO_3^{-2} in the system containing cellulose chain dissolved in NaOH contributes to the increase in entropy upon aggregation of the dissolved chains and drive the system to the stable minimum energy state. This explains the formation of loose aggregates of cellulose chains formed in the experiments when CO_2 is injected into the system [14]. Our results also reveal that the aggregating tendency does not depend upon the interacting sides of the cellulose chains, but only on the presence of carbonate ions in the system.

CRediT authorship contribution statement

Nabin Kumar Karna: Molecular dynamics simulations, Results' analyses, Manuscript preparation. **Alexandra Maria Kozlowski:** Results' analyses, Manuscript preparation. **Merima Hasani:** Conceptualization, Manuscript preparation, Results' analyses.

Declaration of competing interest

The authors declare that they have no known competing financial interests or personal relationships that could have appeared to influence the work reported in this paper.

Data availability

Data will be made available on request.

Acknowledgments

The computations/data handling was enabled by the resources provided by the Swedish National Infrastructure for Computing (SNIC) in NSC at Linköping university partially funded by the Swedish Research Council through grant agreement no. 2018-05973.

Appendix A. Supplementary data

Supplementary material related to this article can be found online at https://doi.org/10.1016/j.chemphys.2023.112060.

References

[1] T. Budtova, P. Navard, Cellulose in NaOH–water based solvents: a review, Cellulose 23 (1) (2016) 5–55.

[2] C. Cuissinat, P. Navard, Swelling and dissolution of cellulose, part III: Plant fibres in aqueous systems, Cellulose 15 (1) (2008) 67–74.

[3] M. Egal, T. Budtova, P. Navard, Structure of aqueous solutions of microcrystalline cellulose/sodium hydroxide below 0 C and the limit of cellulose dissolution, Biomacromolecules 8 (7) (2007) 2282–2287.

[4] P. Navard, C. Cuissinat, Cellulose swelling and dissolution as a tool to study the fiber structure, in: 7th International Symposium "Alternative Cellulose: Manufacturing, Forming, Properties", 2006, 7–pages.

[5] A. Benedetti-Pichler, M. Cefola, Warder's method for the titration of carbonates, Ind. Eng. Chem. Anal. Ed. 11 (6) (1939) 327–332.

[6] S.L. Goertzen, K.D. Thériault, A.M. Oickle, A.C. Tarasuk, H.A. Andreas, Standardization of the boehm titration. Part I. CO2 expulsion and endpoint determination, Carbon 48 (4) (2010) 1252–1261.

[7] J. Schönherr, J.R. Buchheim, P. Scholz, P. Adelhelm, Boehm titration revisited (part i): Practical aspects for achieving a high precision in quantifying oxygen-containing surface groups on carbon materials, C 4 (2) (2018) 21.

[8] P. Sipos, P. May, G. Hefter, Carbonate removal from concentrated hydroxide solutions, Analyst 125 (5) (2000) 955–958.

[9] M. Gunnarsson, D. Bernin, Å. Östlund, M. Hasani, The CO 2 capturing ability of cellulose dissolved in NaOH (aq) at low temperature, Green Chem. 20 (14) (2018) 3279–3286.

[10] M. Gunnarsson, D. Bernin, M. Hasani, The CO 2/CO 3 2- chemistry of the NaOH (aq) model system applicable to cellulose solutions, Cellulose 27 (2020) 621–628.

[11] W. Hempel, J. Seidel, Über verbindungen des kohlendioxyds mit wasser, aethyläther und alkoholen, Ber. Dtsch. Chem. Ges. 31 (3) (1898) 2997–3001.

[12] M. Siegfried, S. Howwjanz, Über die Bindung von Kohlensäure durch Alkohole, Zucker und Oxysäuren, Z. Physiol. Chem. 59 (1909) 376–404.

[13] M. Gunnarsson, D. Bernin, M. Hasani, M. Lund, E. Bialik, Direct evidence for reaction between cellulose and CO2 from nuclear magnetic resonance, ACS Sustain. Chem. Eng. 9 (42) (2021) 14006–14011, http://dx.doi.org/10.1021/acssuschemeng.1c05863.

[14] A.M. Kozlowski, M. Hasani, Cellulose interactions with CO2 in NaOH(aq): The (un)expected coagulation creates potential in cellulose technology, Carbohydr. Polymers 294 (2022) 119771, http://dx.doi.org/10.1016/j.carbpol.2022.119771, URL: https://www.sciencedirect.com/science/article/pii/S0144861722006762.

[15] G. Reyes, R. Ajdary, E. Kankuri, J.J. Kaschuk, H. Kosonen, O.J. Rojas, Cellulose gelation in NaOH (aq) by CO2 absorption: Effects of holding time and concentration on biomaterial development, Carbohydr. Polymers 302 (2023) 120355.

[16] G. Reyes, A.W. King, T.V. Koso, P.A. Penttilä, H. Kosonen, O.J. Rojas, Cellulose dissolution and gelation in NaOH (aq) under controlled CO 2 atmosphere: supramolecular structure and flow properties, Green Chem. 24 (20) (2022) 8029–8035.

[17] N.K. Karna, J. Wohlert, A. Liden, T. Mattsson, H. Theliander, Wettability of cellulose surfaces under the influence of an external electric field, J. Colloid Interface Sci. 589 (2021) 347–355, http://dx.doi.org/10.1016/j.jcis/2021.01.003.

[18] S. Paavilainen, T. R'og, I. Vattulainen, Analysis of twisting of cellulose nanofibrils in atomistic molecular dynamics simulations, J. Phys. Chem. B 115 (14) (2011) 3747–3755, http://dx.doi.org/10.1021/jp111459b.

[19] S. Kishani, T. Benselfelt, L. Wårberg, J. Wohlert, Entropy drives the adsorption of xyloglucan to cellulose surfaces - A molecular dynamics study, J. Colloid Interface Sci. 588 (2021) 485–493, http://dx.doi.org/10.1016/j.jcis.2929.12.113.

[20] M.J. Abraham, T. Murtola, R. Schulz, S. Páll, J.C. Smith, B. Hess, E. Lindahl, GROMACS: High performance molecular simulations through multi-level parallelism from laptops to supercomputers, SoftwareX 1–2 (2015) 19–25.

[21] G. Bussi, D. Donadio, M. Parrinello, Canonical sampling through velocity rescaling, J. Chem. Phys. 126 (1) (2007) 014101, http://dx.doi.org/10.1063/1.2408420.

[22] H.J.C. Berendsen, J.P.M. Postma, W.F. van Gunsteren, A. DiNola, J.R. Haak, Molecular dynamics with coupling to an external bath, J. Chem. Phys. 81 (8) (1984) 3684.

[23] N.J. English, J.M.D. MacElroy, Hydrogen bonding and molecular mobility in liquid water in external electromagnetic fields, J. Chem. Phys. 119 (22) (2003) 11806–11813, http://dx.doi.org/10.1063/1.1624363.

[24] N.J. English, C.J. Waldron, Perspectives on external electric fields in molecular simulation: progress, prospects and challenges, Phys. Chem. Chem. Phys. 17 (2015) 12407–12440.

[25] Z. Futera, N.J. English, Communication: Influence of external static and alternating electric fields on water from long-time non-equilibrium ab initio molecular dynamics, J. Chem. Phys. 147 (3) (2017) 031102, http://dx.doi.org/10.1063/1.4994694.

[26] Y. Nishiyama, P. Langan, H. Chanzy, Crystal structure and hydrogen-bonding system in cellulose Iβ from synchroton X-ray and neutron fiber diffraction, J. Am. Chem. Soc. 124 (31) (2002) 9074–9082, http://dx.doi.org/10.1021/ja0257319.

[27] V. Hornak, R. Abel, A. Okur, B. Strockbine, A. Roitberg, C. Simmerling, Comparison of multiple amber force fields and development of improved protein backbone parameters, Proteins Struct. Funct. Bioinform. 65 (3) (2006) 712–725.

[28] J. Huang, S. Rauscher, G. Nawrocki, T. Ran, M. Feig, B.L. de Groot, H. Grubmuller, A.D. MacKerell, CHARMM36m: an improved force field for folded and intrinsically disordered proteins, Nature Methods 14 (2017) 71–73.

[29] L. Pol Fachin, V.H. Rusu, H. Verli, R.D. Lins, GROMOS 53A6GLYC, an improved GROMOS force field for hexopyranose-based carbohydrates, J. Chem. Theory Comput. 8 (11) (2012) 4681–4690, http://dx.doi.org/10.1021/ct300479h, PMID: 26605624.

[30] M. Bergenstråhle, L.A. Berglund, K. Mazeau, Thermal response in crystalline I cellulose: A molecular dynamics study, J. Phys. Chem. B 111 (30) (2007) 9138–9145.

[31] H.J.C. Berendsen, J.R. Grigera, T.P. Straatsma, The missing term in effective pair potentials, J. Phys. Chem. 91 (1987) 6269–6271.

[32] B. Stenqvist, E. Wernersson, M. Lund, Cellulose-water interactions: Effect of electronic polarizability, Nordic Pulp Paper Res. J. 30 (1) (2015) 26–31.

[33] J. Schmidt, S. Roberts, J. Loparo, A. Tokmakoff, M. Fayer, J. Skinner, Are water simulation models consistent with steady-state and ultrafast vibrational spectroscopy experiments? Chem. Phys. 341 (1) (2007) 143–157, http://dx.doi.org/10.1016/j.chemphys.2007.06.043, URL: http://www.sciencedirect.com/science/article/pii/S0301010407002418. Ultrafast Dynamics of Molecules in the Condensed Phase: Photon Echoes and Coupled Excitations.

[34] C. Vega, E. de Miguel, Surface tension of the most popular models of water by using the test-area simulation method, J. Chem. Phys. 126 (15) (2007) 154707, http://dx.doi.org/10.1063/1.2715577.

[35] D. Boda, D. Henderson, The effects of deviations from Lorentz-Berthelot rules on the properties of a simple mixture, Mol. Phys. 106 (20) (2008) 2367–2370.

[36] S. Kumar, J.M. Rosenberg, D. Bouzida, R.H. Swendsen, P.A. Kollman, Multidimensional free-energy calculations using the weighted histogram analysis method, J. Comput. Chem. 16 (11) (1995) 1339–1350, http://dx.doi.org/10.1002/jcc.540161104, URL: https://onlinelibrary.wiley.com/doi/abs/10.1002/jcc.540161104.

[37] M. in Het Panhuis, C.H. Patterson, R.M. Lynden-Bell, A molecular dynamics study of carbon dioxide in water: diffusion, structure and thermodynamics, Mol. Phys. 94 (6) (1998) 963–972, http://dx.doi.org/10.1080/002689798167539.

[38] R. Pohorecki, W. Moniuk, Kinetics of reaction between carbon dioxide and hydroxyl ions in aqueous electrolyte solutions, Chem. Eng. Sci. 43 (7) (1988) 1677–1684, http://dx.doi.org/10.1016/0009-2509(88)85159-5, URL: https://www.sciencedirect.com/science/article/pii/0009250988851595.

[39] P. Chen, G. Lo Re, L.A. Berglund, J. Wohlert, Surface modification effects on nanocellulose – molecular dynamics simulations using umbrella sampling and computational alchemy, J. Mater. Chem. A 8 (2020) 23617–23627, http://dx.doi.org/10.1039/D0TA09105G.